A simple retrieval method of land surface temperature from AMSR-E passive microwave data—A case study over Southern China during the strong snow disaster of 2008

Shui-sen Chen [a,b,*], Xiu-zhi Chen [a,b,c], Wei-qi Chen [d], Yong-xian Su [a,b,c], Da Li [a,b,c]

[a] Guangzhou Institute of Geochemistry, CAS, Guangzhou 510070, China
[b] Guangzhou Institute of Geography, Guangzhou 510070, China
[c] Graduate School of Chinese Academy of Sciences, Beijing 100049, China
[d] Department of Geography, Florida State University, Tallahassee, FL 32304, USA

ARTICLE INFO

ABSTRACT

The analysis of the passive microwave radiance transfer equation certifies that there is a linear relationship between satellite-generated brightness temperatures (BT) and in situ observation temperature and that land surface temperature (LST) is largely influenced by vegetation cover conditions. Microwave polarization difference index (MPDI) is an effective indicator for characterizing the land surface vegetation cover density. Based on the analysis of LST models from AMSR-E BT with 6.9 GHz MPDI intervals at 0.04, 0.02 and 0.01, respectively, this paper developed a simplified LST regression model with MPDI-based five land cover types, combining observation temperatures from 86 meteorological observation stations. The study shows that smaller MPDI intervals can obtain higher accuracy of AMSR-E LST simulation, and that the combination of HDF Explorer and ArcGIS software was useful for automatically processing the pixel latitude, longitude and BT information from the AMSR-E HDF imagery files. The RMSE of the five LST simulation algorithms is between 1.47 and 1.92 °C, with an average LST retrieval error of 0.91–1.30 °C. Besides, only 7 polarization bands and 5 land surface types are required by the proposed simplified model. The new LST simulation models appears to be more effective for producing LST compared to past most studies, of which the accuracy used to be more than 2 °C. This study is one of the rare applications that combine the meteorological observation temperature with MPDI to produce the LST regression analysis algorithms with less RMSE from AMSR-E data. The results can be referred to similar areas of the world for LST retrieval or land surface process research, in particular under extreme bad weather conditions.

© 2010 Elsevier B.V. All rights reserved.

1. Introduction

Since 1990, five strong cold disasters have occurred in Guangdong Province of Southern China, causing serious economic losses (Wang et al., 2004). In 2008, another strong snow disaster attacked the province again, which is one of the worst storms of the past 50 years. As a result, timely acquirement of regional temperature information on a large scale is becoming more and more urgent for emergency management in such situations. This has recently made the remote sensing of land surface temperature (LST) an important research subject in China. Many methodologies have been established to retrieve LST from thermal infrared satellite sensor data (Mao et al., 2007a,b). However, the thermal remote sensing is greatly influenced by cloud, atmospheric water content and rainfall. Therefore, thermal remote sensing from optical sensors cannot be used to retrieve LST during the periods of cold disasters or under other bad weather conditions. Microwave remote sensing can just overcome these disadvantages. Passive microwave emission can penetrate non-precipitating clouds, thereby providing a better representation of LST under nearly all sky conditions. What is more, daily data are available from microwave radiometers as compared to optical sensors like Landsat[TM], ASTER or MODIS of which only weekly series products are available. The coarse spatial resolution of passive microwave remote sensing is not a problem for large scale studies and therefore providing nearly 20-year time series by now, which are of great interest for recent climate change studies (Fily et al., 2003).

Passive microwave remote sensing has already been used to retrieve LST for almost 20 years. McFarland et al. (1990) made some significant conclusions: LST for crop/range, moist soils, and dry soils surface types can be retrieved with linear regression models from passive microwave SSMI/I brightness temperatures (BT). The BT of SSMI/I 85 GHz vertical polarization is the primary channel for LST

correlation. The 19 GHz band can compensate for the influence of surface water. The difference between 37 and 22 GHz can be utilized to correct the influence of atmospheric water vapor content on the emission. Njoku (1993) found that neural network method was more appropriate for developing a useful LST retrieval algorithm. Multi-channel measurements can estimate and correct the surface emissivity and atmospheric effects. They also established a nonlinear retrieval algorithm, with an accuracy that can reach 2–2.5 °C. Njoku and Li (1997) also used the satellite microwave radiometer data at the range of 6–18 GHz frequency to derive LST. A surface temperature accuracy of 2 °C was achievable, except for bare soils where discrimination between moisture and temperature variability is difficult using this algorithm. Aires et al. (2001) developed a new neural network and variant assimilation method, and the theoretical RMSE of LST retrieval over globe is 1.3 K in clear-sky conditions and 1.6 K in cloudy scenes.

However, the passive microwave retrieval algorithm of LST from AMSR-E BT is rarely seen in the present stage of application of passive microwave radiometry in China. Mao et al. (2007a,b) established a regression analysis model between the BT of the AMSR-E bands and MODIS LST products. The average retrieval LST error is about 2–3 °C relative to the MODIS LST products. He also found that the 89 GHz vertical polarization is the best single band to retrieve MODIS LST. However, over 60% of the areas in MODIS LST product are influenced by weather, especially cloud. The MODIS LST itself contains certain errors when the air contains much cloud, atmospheric water content or rainfall. So the regression model between AMSR-E BT and MODIS LST products lacks some practical significance. Our objective here is to establish a regression model between AMSR-E BT and observation temperatures (Ts) from meteorological observation stations over Guangdong Province and to describe a new, simple, yet still efficient algorithm to derive LST under bad weather conditions during the snow disaster of Southern China in 2008. Further more, the ground emissivity has a considerable impact on the accuracy of retrieved LST from remote sensing data (Rubio et al., 1997; Yang and Yang, 2006), and it is also influenced by land surface cover conditions, such as the density of vegetation cover and soil moisture levels. This paper aims to develop such a regression model based on different degrees of vegetation cover.

2. Study data, area and method

2.1. Study data and area

The AMSR-E instrument on the NASA Earth Observing System (EOS) Aqua satellite is a modified version of the AMSR instrument launched on the Japanese Advanced Earth Observing Satellite-II (ADEOS-II) in 1999. AMSR-E is a successor in technology to the Scanning Multi-channel Microwave Radiometer (SMMR) and Special Sensor Microwave Imager (SSM/1) instruments, first launched in 1978 and 1987, respectively. It provides global passive microwave measurements of terrestrial, oceanic, and atmospheric variables for the investigation of global water and energy cycles. The daily AMSR-E BT products during the period of January 25, 2008 to February 5, 2008 were downloaded from the website of National Snow and Ice Data Center (NSIDC) and used in this study. The imagery dates (Beijing time—Eastern Eight Zone) are: January 25 (02 h:06 min, 12 h:48 min), January 26 (13 h:32 min), January 27 (01 h:53 min), January 28 (13 h:19 min), January 29 (01 h:41 min), January 30 (13 h:07 min), February 1 (02 h:12 min, 12 h:55 min), February 3 (02 h:00 min), February 4 (13 h:26 min) and February 5 (01 h:47 min). They contain BT at 6.9, 10.7, 18.7, 23.8, 36.5, and 89.0 GHz. Data are resampled to be spatially consistent, and therefore are available at a variety of resolutions that correspond to the

sizes of footprints of the observations such as 56, 38, 24, 21, and 12 km, respectively. The spatial characters of the AMSR-E products are given in Table 1.

Guangdong Province, a coastal province, located in Southern China, with a population of 86,420,000 people and area of 177,900 km², was chosen as the study area (Fig. 1). It is a key center of China on manufacturing, transportation, and import and export trade. During the period of the 2008 serious snow disaster in China, an unprecedented cold disaster attacked Guangdong Province. During the disaster, much of the crops and trees there were damaged and thousands of passengers and cars were blocked on high ways. Even worse, in some areas, the electrical wire was disconnected. It caused direct economic losses of about 150 billion RMB in China (http://www.mca.gov.cn). Retrieving the LST from microwave remote sensing data is conducive to establishing a microwave monitoring database of cold disasters and is also useful for government decision-making for future cold disaster preparedness. It is necessary to study on the event using all-weather microwave remote sensing monitoring. There are 86 meteorological observation stations (triangle points in Fig. 1) in Guangdong Province that correspond to the times of AMSR-E imageries used in the model development and leave-one-out cross-validation. The average time difference of in situ meteorological observation and AMSR-E imageries is 9 min (0–19 min). The daily Ts data (from January 25, 2008 to February 5, 2008), which were used to build the regression model with the AMSR-E BT in this paper, were provided by Meteorology Bureau of Guangdong Province.

2.2. Method

2.2.1. Theoretical basis of LST retrieval from AMSR-E data

Compared to the thermal radiance transfer equation, ground emissivity must be considered in the passive microwave radiance transfer equation. Atmosphere also has important effects on the received radiance at a remote sensing sensor level. Taking into account the two impacts, the general radiance transfer equation for passive microwave remote sensing of LST can be formulated as (Mao et al., 2007a,b):

$$B_f(T_f) = \tau_f(\theta)\varepsilon_f B_f(T_{\text{soil}}) + [1 - \tau_f(\theta)](1 - \varepsilon_f)\tau_f(\theta)B_f(T_a^\downarrow)$$
$$+ [1 - \tau_i(\theta)]B_f(T_a^\uparrow) \tag{1}$$

where T_f is the BT in frequency f, T_{soil} is the average soil temperature, T_a is the average atmosphere temperature, $B_f(T_{\text{soil}})$ is the ground radiance, $B_f(T_a^\downarrow)$ and $B_f(T_a^\uparrow)$ are the downwelling and upwelling path radiance, respectively, $\tau_f(\theta)$ is the atmosphere transmittance in frequency f at viewing direction θ (zenith angle from nadir), and ε_f is the ground emissivity.

Planck's function (expression (A1) in Appendix A) describes the relationship between spectral radiance emitted by a black body and real temperature. On the basis of the Taylor series expansion expression, Planck's function can be written as expression (A2) (Appendix A). What is more, as to the AMSR-E, the frequencies of the microwave bands are 6.9, 10.7, 18.7, 23.8, 36.5, and 89.0 GHz. And the LST of Guangdong Province from January 25, 2008 to February 5, 2008 are all greater than −10 °C (bigger than 263 K). Therefore, the value of the term hf/kT can be assumed to be zero. Hence Planck's function can be simplified as expression (A3) (Appendix A). Then, Eq. (1) can be simplified as

$$T_f = \tau_f\varepsilon_f T_{\text{soil}} + (1 - \tau_f)(1 - \varepsilon_f)\tau_f T_a^\downarrow + (1 - \tau_i)T_a^\uparrow \tag{2}$$

From Eq. (2) we can clearly find that there is a linear relationship between remote sensing BT and LST. We can establish a linear regression model to retrieve LST from microwave BT.

Furthermore, we assume that a vegetation layer can be considered as a plane, parallel, absorbing, and scattering medium at a

Table 1
Spatial characteristics of AMSR-E products.

Footprint size	Mean spatial resolution	Channels (GHz)					
		89.0	36.5	23.8	18.7	10.7	6.9
75 km × 43 km	56 km	Δ	Δ	Δ	Δ	Δ	Δ
51 km × 29 km	38 km	Δ	Δ	Δ	Δ	Δ	
27 km × 16 km	21 km	Δ	Δ	Δ			
14 km × 8 km	12 km	Δ					

Δ: Means including the corresponding AMSR-E channel.
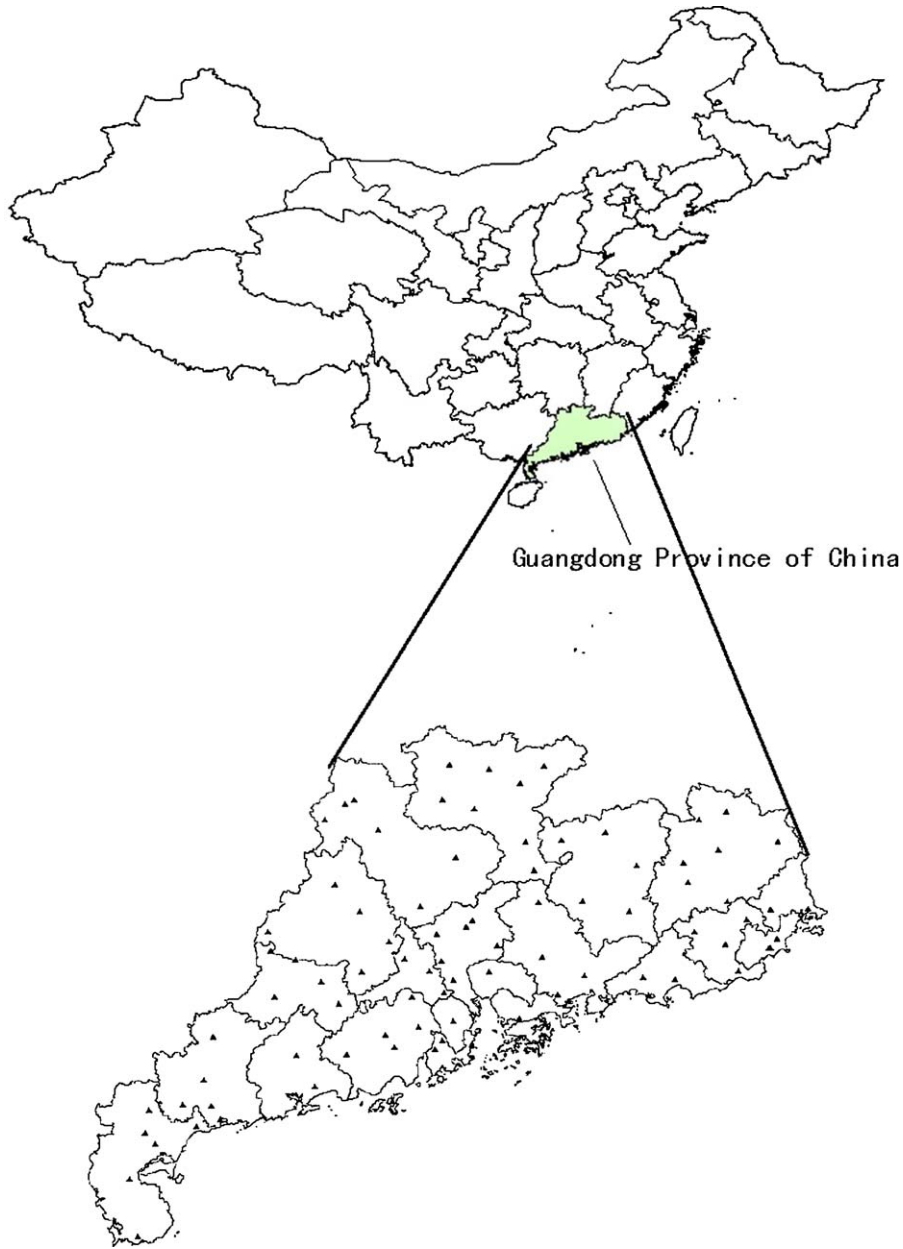
Fig. 1. Study area and 86 meteorological observation stations in Guangdong Province.

constant temperature T_c upon the soil surface. The brightness temperature $T_p(\tau,\mu)$ of the radiation emitted by vegetation canopy at an angle θ from the zenith can be written as follows (Paloscia and Pampaloni, 1988):

$$T_p(\tau, \mu) = (1 - w)(1 - e^{-\tau/\mu})T_c + \varepsilon_p T_{\text{soil}} e^{-\tau/\mu} \qquad (3)$$

where p stands for horizontal (H) or vertical (V) polarization, $\mu = \cos\theta$. τ is the equivalent optical depth, w is the single scattering albedo. The two parameters can characterize the absorbing and scattering properties of vegetation, respectively. ε_p is the soil emissivity for the p polarization.

Microwave polarization difference index (MPDI) (expression (A4) in Appendix A) is an effective indicator for characterizing the
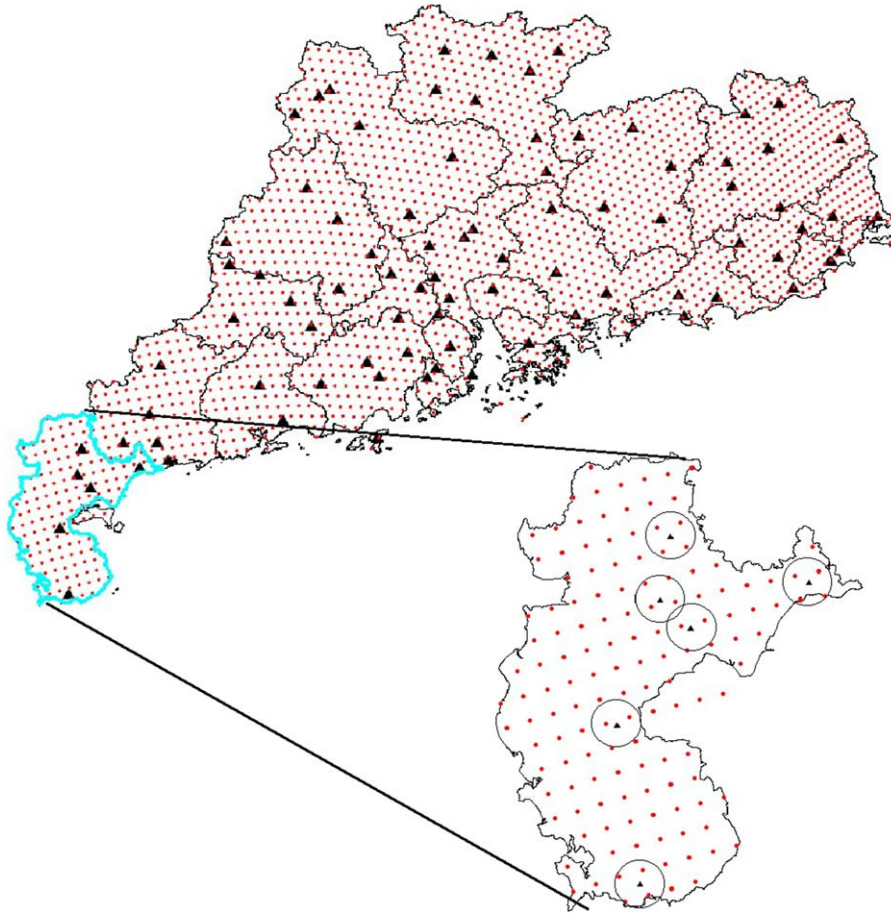
Fig. 2. An example explaining the method of matching the imagery pixels' BT against Ts of 86 meteorological observation stations within Guangdong Province.

land surface vegetation cover density. Using Eq. (3), MPDI used in the study can be described as

$$\text{MPDI}(\tau, \mu) = \frac{(\varepsilon_V T_{\text{soil V}} - \varepsilon_H T_{\text{soil H}})e^{-\tau/\mu}}{2(1-w)(1-e^{-\tau/\mu})T_c + (\varepsilon_V T_{\text{soil V}} - \varepsilon_H T_{\text{soil H}})e^{-\tau/\mu}} \tag{4}$$

When there is little vegetation cover over the land surface, the value of τ can be defined as zero. So the MPDI of bare ground can be written as expression (A5) (Appendix A).

According to Paloscia and Pampaloni (1988), we can assume $\varepsilon_{\text{soil}}(\varepsilon_V + \varepsilon_H)/2$, and $T_c = T_{\text{soil}}$. Then Eq. (4) can be further simplified as

$$\text{MPDI}(\tau, \mu) \approx \text{MPDI}(0, \mu)e^{-\tau/\mu} \tag{5}$$

Obviously from Eq. (5), MPDI mainly depends on μ and τ, and MPDI value falls as vegetation becomes thicker. Therefore, MPDI can indicate the density of land surface vegetation cover. LST is also influenced greatly by vegetation cover condition. Thus, we classify the land surface vegetation cover conditions into several types based on the values of MPDI.

What is more, as the frequency of microwave band becomes higher, the value of τ rises, and the MPDI values fall correspondingly. MPDI of a lower frequency channel is more effective to reflect the land surface vegetation cover conditions. Therefore, we produced the MPDI imageries using 6.9 GHz horizontal and vertical polarization BT. At last, we developed regression LST retrieval algorithms for each land surface type, respectively.

2.2.2. Match microwave BT against observation temperature (Ts)

Since Ts of 86 meteorological observation stations are point-based, we carried out appropriate processing to calculate the imagery-pixel BT using nearest pixel temperature or averaged pixel temperature within the circle of a radius 9,000 m around the meteorological observation stations (Fig. 2), because the cycle radius of 9,000 m can just include three or four imagery pixels for acquirement of average BT. At first, we downloaded AMSR-E BT data from ftp://n4ftl01u.ecs.nasa.gov. The original file type is HDF. We used HDF Explorer software to extract latitude, longitude and BT information from the HDF files, and saved them into separate text files. Then, ArcGIS was used to read the latitude, longitude and BT information and display them. About 2,223 pixels were extracted from each AMSR-E BT file within Guangdong Province (black dots in Fig. 2). Then we drew 86 circles centralized at each meteorological observation station, containing three or four BT pixels within each circle. The average values of pixels' BT that included in the circle were used to make linear regression analysis with Ts (given in Fig. 2).

2.2.3. Technical diagram of the study

The simple procedure of LST retrieval is given in Fig. 3. We first calculate MPDI of Guangdong Province using the AMSR-E 6.9 GHz BT. Then we classified the land surface cover types of Guangdong Province based on different values of MPDI. Three classification methods were implemented in this study at the MPDI intervals of 0.04, 0.02, and 0.01, respectively.

After that, we developed three retrieval models, Model 1, 2 and 3 from AMSR-E BT data at MPDI (6.9 GHz) intervals of 0.04, 0.02
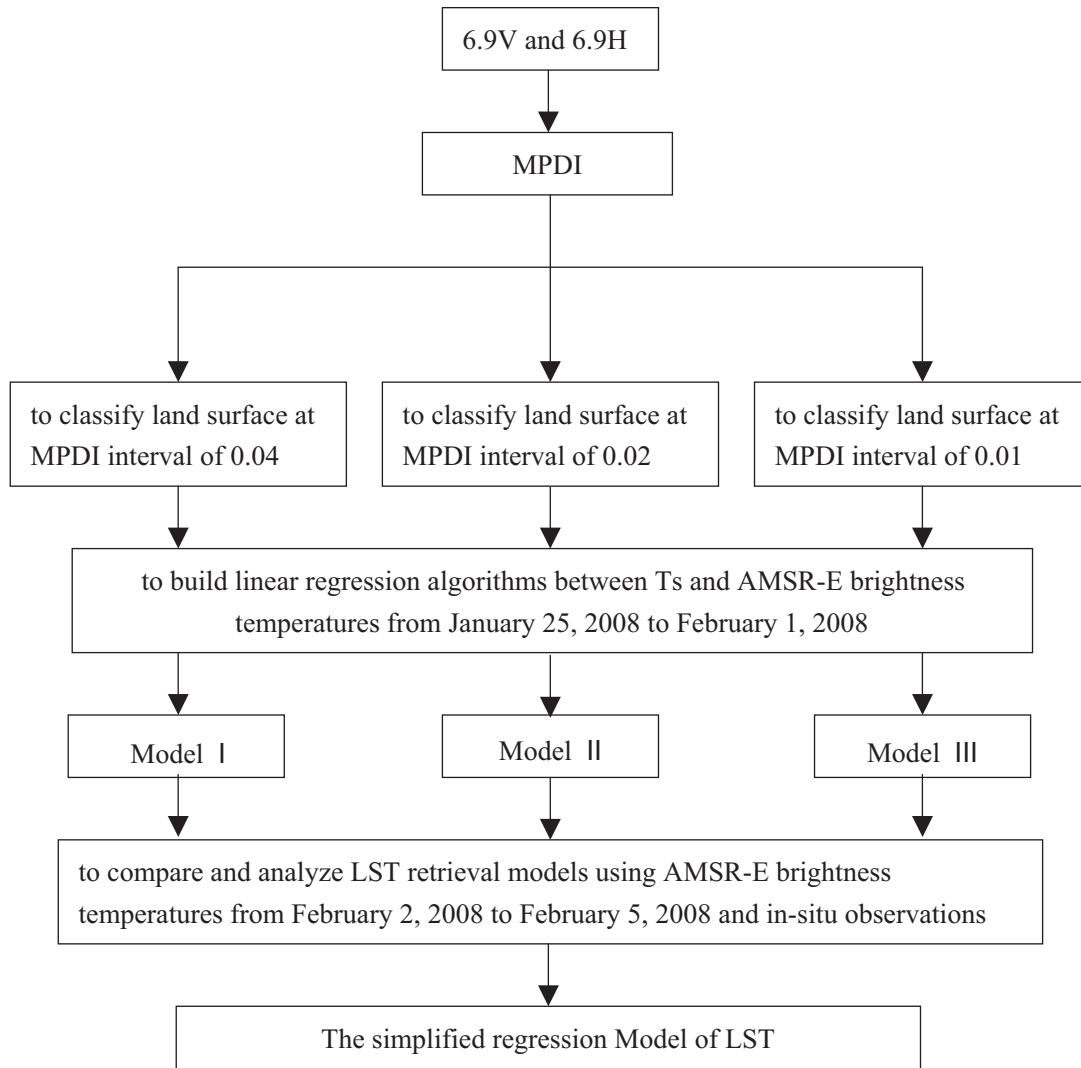
Fig. 3. Procedure of LST retrieval from AMSR-E BT data in the study.

Table 2
Linear regression algorithms of Model 1 (the interval of MPDI is 0.04). H: horizontal polarization; V: vertical polarization.

Range of MPDI	Equation	R^2	Accuracy evaluated by cross-validation	
			RMSE (°C)	Average LST error (°C)
<0.04	LST = 0.00060 × 6.9H + 0.00183 × 10.7H + 0.01867 × 18.7V − 0.01379 × 18.7H − 0.00282 × 36.5V + 0.00321 × 36.5H − 0.00005 × 89H + 53.7612	0.782	1.61	1.23
0.04–0.08	LST = 0.00124 × 6.9V − 0.00481 × 10.7V + 0.00210 × 10.7H + 0.02118 × 18.7V − 0.01204 × 18.7H + 0.00113 × 23.8H + 57.3844	0.686	1.68	1.21
0.08–0.12	LST = 0.00060 × 6.9H − 0.00923 × 10.7V + 0.00425 × 10.7H + 0.02804 × 18.7V − 0.01434 × 18.7H + 63.87276	0.797	1.81	2.53

Table 3
Linear regression algorithms of Model 2 (the interval of MPDI is 0.02).

Range of MPDI	Equation	R^2	Accuracy evaluated by cross-validation	
			RMSE (°C)	Average LST error (°C)
<0.02	LST = 0.00359 × 10.7H + 0.01649 × 18.7V − 0.01378 × 18.7H + 0.00113 × 36.5H − 0.00006 × 89H + 52.63216	0.771	1.60	1.25
0.02–0.04	LST = 0.00097 × 6.9H + 0.00143 × 10.7H + 0.02295 × 18.7V − 0.01558 × 18.7H + 0.00171 × 36.5H − 0.00114 × 89V + 69.92912	0.812	1.37	1.09
0.04–0.06	LST = 0.00161 × 6.9V − 0.00189 × 10.7V + 0.01843 × 18.7V − 0.01064 × 18.7H + 0.00324 × 36.5V − 0.00097 × 89V + 62.70204	0.783	1.36	1.03
0.06–0.08	LST = 0.01373 × 23.8V − 0.00661 × 23.8H + 48.36916	0.477	2.22	1.70
0.08–0.10	LST = 0.01490 × 23.8V − 0.00746 × 2.38H + 49.94792	0.515	2.45	1.84
0.10–0.12	LST = −0.00604 × 10.7V + 0.00428 × 10.7H + 0.02609 × 18.7V − 0.01472 × 18.7H + 63.88248	0.881	1.47	1.15
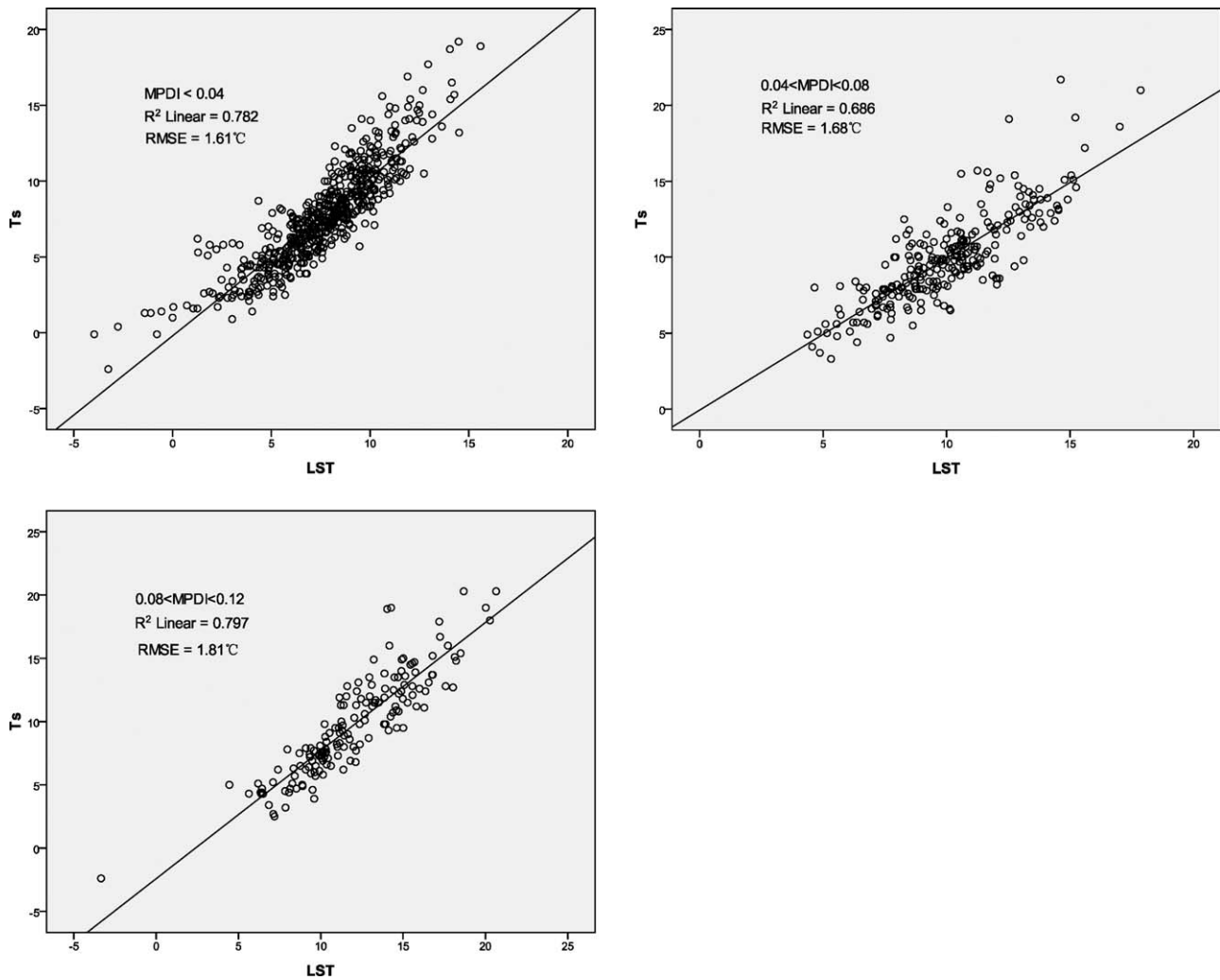
Fig. 4. Correlation analysis between LST retrieved from AMSR-E BT and Ts (the interval of MPDI is 0.04).

and 0.01, respectively, to derive LST of study area from January 25, 2008 to February 5, 2008.

Considering that the above three Models are complicated with low accuracy at the MPDI range of 0.6–0.9. In order to product more accurate LST retrieval models when the range of MPDI interval becomes smaller, a new land surface vegetation cover classifica-

tion rule is proposed as follows: when MPDI is smaller than 0.06, land surface was seen as the same land vegetation cover type (being covered with dense vegetation); when MPDI is between 0.06 and 0.09 (land surface being covered with sparse vegetation mixed with bare soil), the land surface was further classified into three types (MPDI: 0.06–0.07; 0.07–0.08; 0.08–0.09) according to the new land

Table 4
Linear regression algorithms of Model 3 (the interval of MPDI is 0.01).

Range of MPDI	Equation	R^2	Accuracy evaluated by cross-validation	
			RMSE (°C)	Average LST error (°C)
<0.01	$LST = 0.00494 \times 6.9H + 0.00395 \times 23.8V + 64.77052$	0.751	1.70	0.90
0.01–0.02	$LST = 0.00313 \times 10.7H + 0.01626 \times 18.7V - 0.01314 \times 18.7H + 0.00151 \times 23.8H + 54.51868$	0.763	1.54	1.06
0.02–0.03	$LST = 0.00142 \times 6.9H + 0.02101 \times 18.7V - 0.01315 \times 18.7H + 0.00382 \times 36.5V - 0.00158 \times 89H + 75.82136$	0.846	1.24	0.88
0.03–0.04	$LST = 0.00082 \times 6.9V + 0.02021 \times 18.7V - 0.01110 \times 18.7H + 64.53724$	0.798	1.59	0.90
0.04–0.05	$LST = 0.00199 \times 6.9V + 0.01495 \times 18.7V - 0.01136 \times 18.7H + 0.00481 \times 23.8V - 0.00141 \times 89V + 58.03964$	0.833	1.26	0.89
0.05–0.06	$LST = 0.00104 \times 6.9V - 0.00390 \times 10.7V + 0.02206 \times 18.7V - 0.00955 \times 18.7H + 61.5722$	0.755	1.42	0.71
0.06–0.07	$LST = 0.00110 \times 6.9H + 0.00998 \times 36.5V - 0.00457 \times 36.5H + 52.19068$	0.716	1.47	0.91
0.07–0.08	$LST = 0.00122 \times 6.9H + 0.01109 \times 18.7V - 0.00823 \times 18.7H + 0.00500 \times 23.8V + 62.21144$	0.716	1.92	1.10
0.08–0.09	$LST = 0.01496 \times 36.5V - 0.00720 \times 36.5H + 52.18968$	0.757	1.89	1.10
0.09–0.10	$LST = 0.01338 \times 23.8V - 0.00607 \times 23.8H + 50.59308$	0.754	1.85	1.28
0.10–0.11	$LST = 0.00744 \times 10.7V + 55.90692$	0.791	1.48	1.09
0.11–0.12	$LST = 0.209 \times 6.9V + 0.390 \times 89V - 144.236$	0.777	1.98	1.22
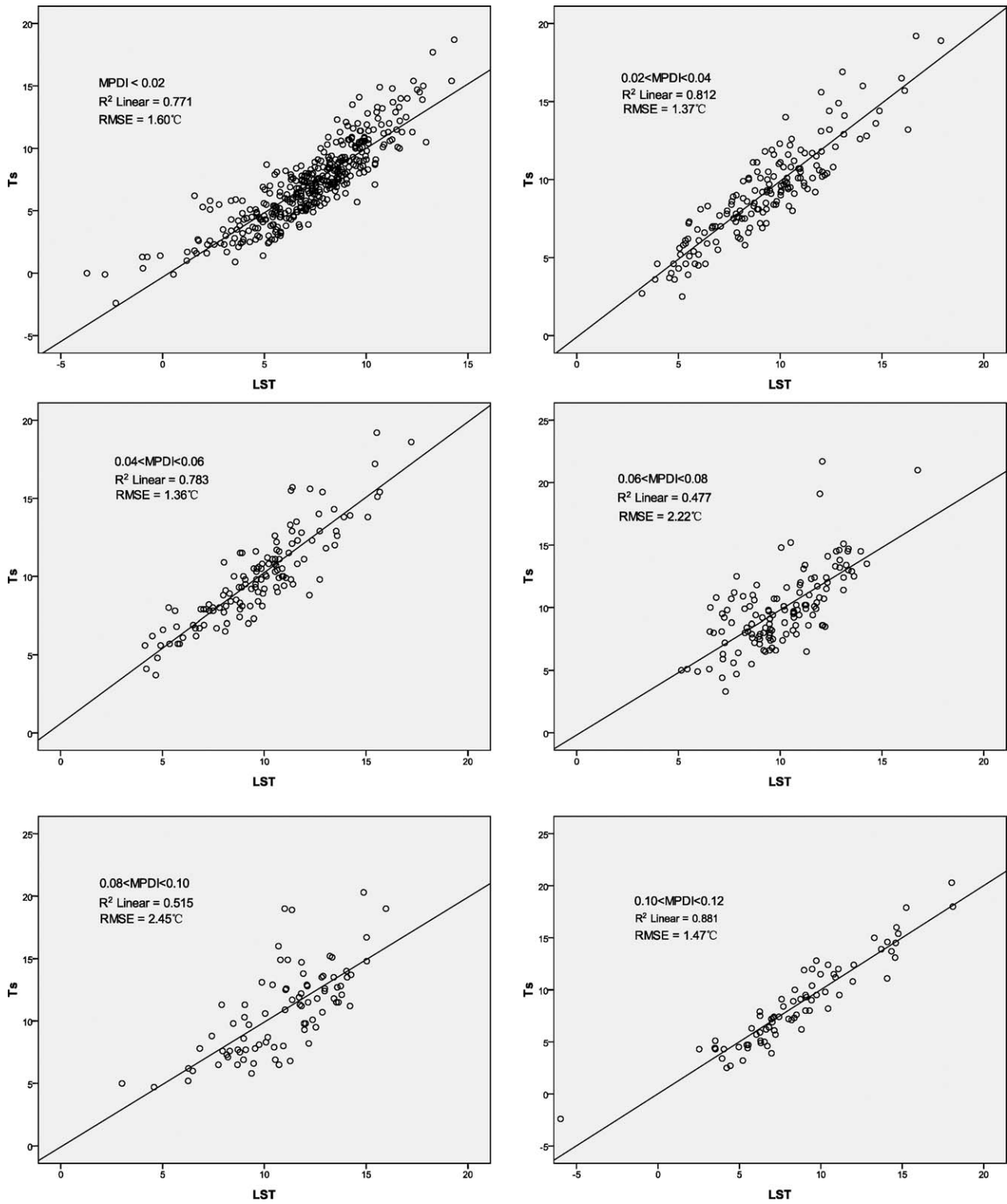
Fig. 5. Correlation analysis between LST retrieved from AMSR-E BT and Ts (the interval of MPDI is 0.02).

surface vegetation cover classification rule; when MPDI is between 0.09 and 0.12, the land surface was defined as bare soil. As the number of areas where the MPDI > 0.12 is few and far between (about 13 of 2,223 pixels in each AMSR-E BT file), there is no statistically significance to built regression algorithms for such areas. So we ignored those areas where MPDI > 0.12. Finally, a simplified LST retrieval model was established based on the new vegetation cover classification rule mentioned above.

3. Results and discussion

3.1. The three LST models with MPDI intervals at 0.04, 0.02 and 0.01

The scatter diagrams were presented to compare the MDPI-based LST retrieved from AMSR-E BT with Ts observed by 86 meteorological observation stations. Average LST errors and RMSE

by leave-one-out cross-validation were used to evaluate the retrieval results of the three models. Detailed descriptions of the three models are as following:

(1) Model 1: We classified the land surface into three types at the MPDI interval of 0.04, and built three linear regression algorithms for each land surface type in total (Fig. 4).

(2) Model 2: On the basis of Model 1, we further classified the land surface into six types at the MPDI interval of 0.02, and developed six linear regression algorithms for each land surface type (Fig. 5).

(3) Model 3: Similarly, we classified the land surface of study area into twelve types at the MPDI interval of 0.01, and established twelve linear regression algorithms for each land surface type correspondingly (Fig. 6a and b).
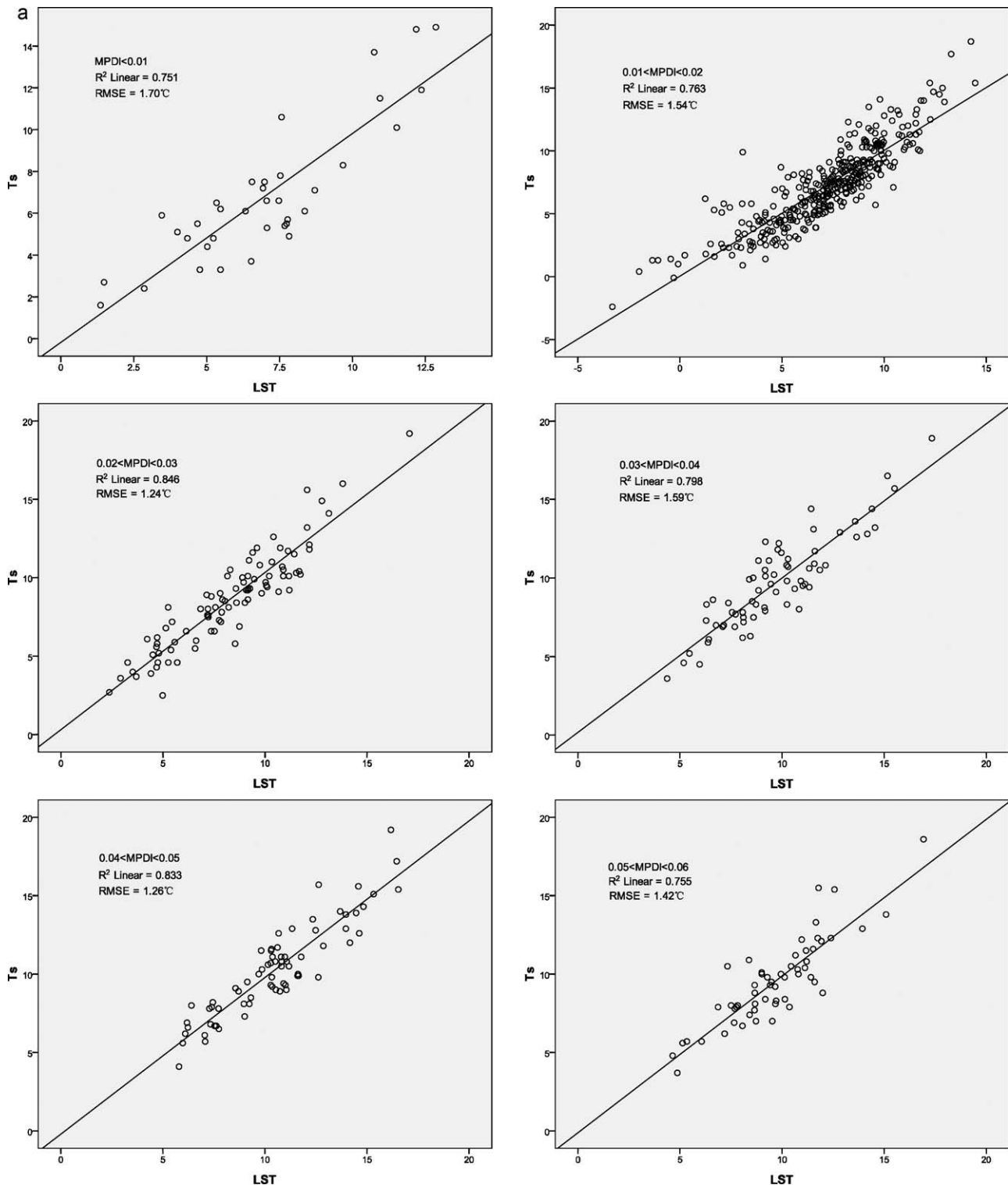
Fig. 6. (a) Correlation analysis between LST retrieved from AMSR-E BT and Ts (the interval of MPDI is 0.01); (b) correlation analysis between LST retrieved from AMSR-E BT and Ts (the interval of MPDI is 0.01).
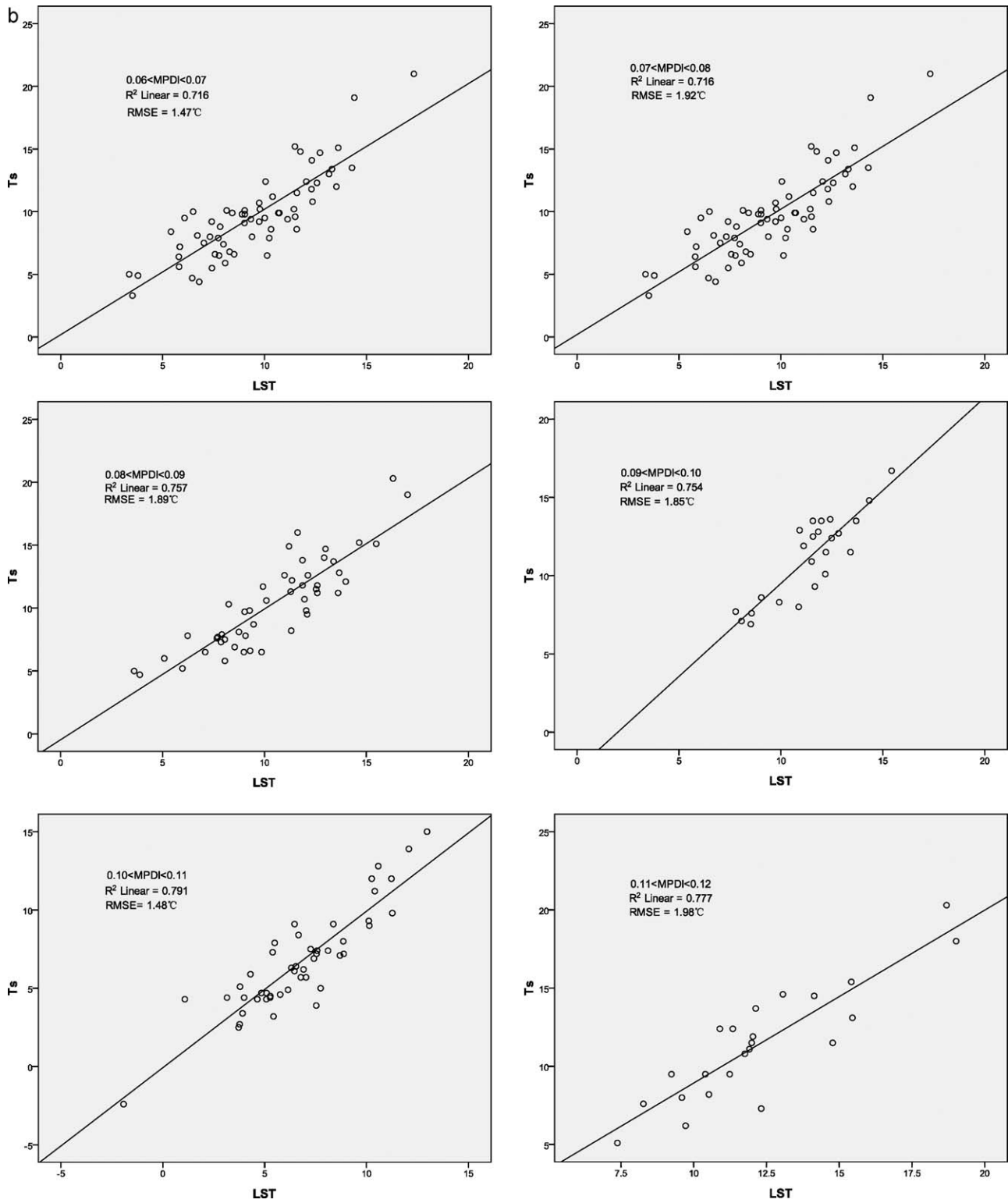
Fig. 6. (*Continued*).

Average temperature errors of Model 1 between Ts and LST are listed in Table 2 and Fig. 4. It clearly showed that when MPDI <0.08 (under dense vegetation cover condition), the LST retrieval algorithm is more effective (smaller average temperature error); when 0.08 < MPDI < 0.12, the average LST Error attains 2.53 °C. However, the RMSE of three regression algorithms are not more than 1.81 °C ($R^2 \geq 0.686$) with average error 0f 1.66 °C.

The analyzed results of Model 2 are given in Table 3 and Fig. 5. It clearly showed that all the LST retrieval algorithms are very effective (LST error range: 1.03–1.84 °C, average error at 1.34 °C) except for the two MPDI range: 0.06–0.08 ($R^2 = 0.477$, RMSE = 2.22) and 0.08–0.10 ($R^2 = 0.515$, RMSE = 2.45). R^2 of the two algorithms are relatively low and RMSE is a little higher than others. The LST retrieval algorithms are only effective under dense vegetation cover
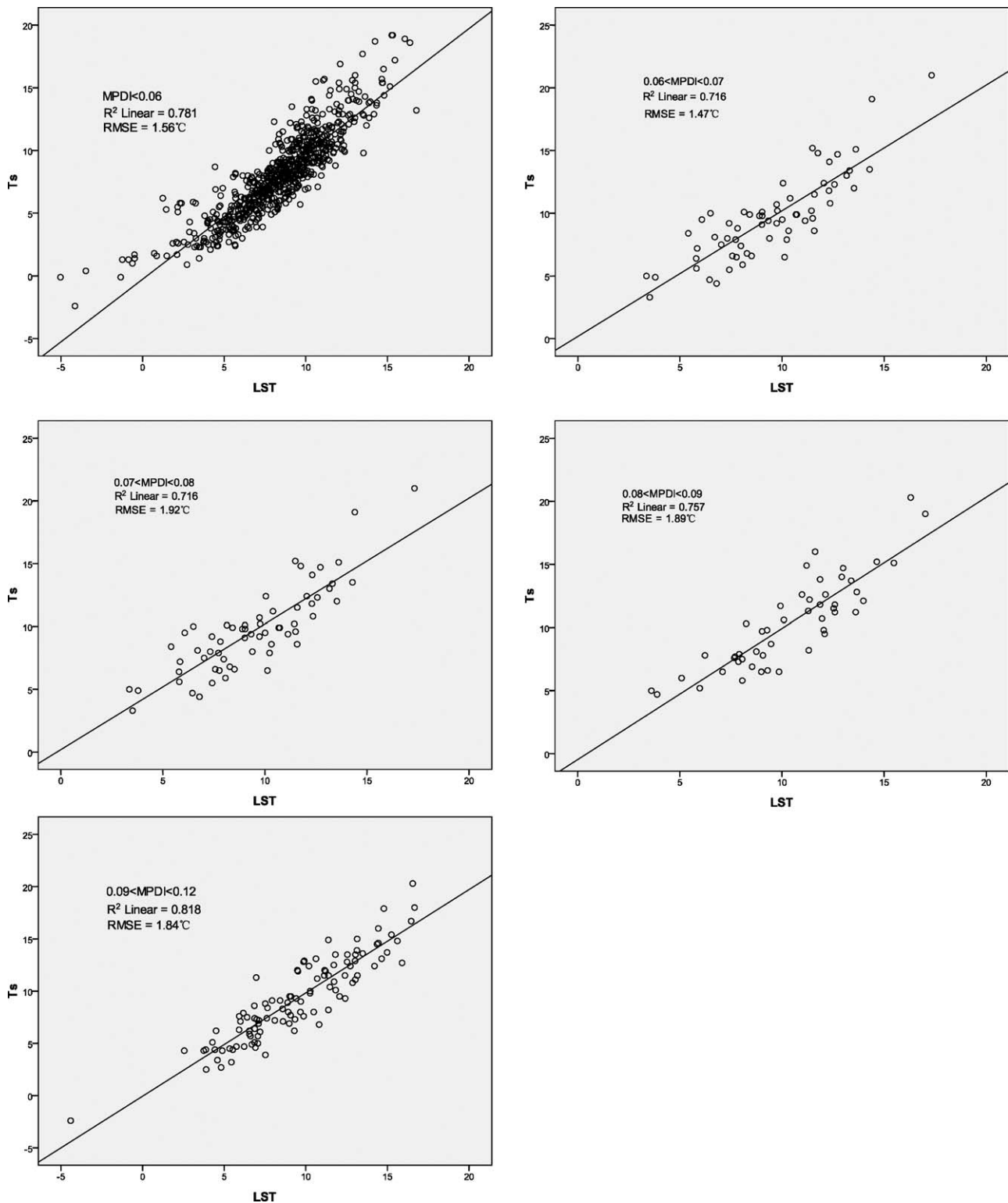
Fig. 7. Comparison of LST retrieved from AMSR-E BT and Ts (final simplified LST retrieval model) (the interval of MPDI is 0.01 at the MPDI range of 0.6–0.9).

and bare soil conditions. On the whole, the RMSE of Model 2 is still within 2.45 °C (1.36–2.45 °C) with average RMSE at 1.75 °C.

The accuracy analysis of Model 3 validated by leave-one-out cross-validation method is given in Fig. 6a and b and Table 4. It clearly showed that all LST algorithms of model 3 are effective with average temperature errors between 0.71 and 1.28 °C (R^2: 0.716–0.846), so the LST retrieval algorithms are more accurate by using smaller MDPI intervals to classify the land surface cover

conditions. The RMSE of regression algorithms are not more than 2.0 °C (1.24–1.98 °C, average RMSE at 1.61 °C), which is better than the former two models' results (Model 1 and Model 2). Only when the MPDI values are more than 0.07, the RMSE of models are more than 1.8 °C (1.85–1.98 °C).

Seen from the above discussions, we note that all the three Models were not perfect. The accuracy levels of Model 1 and Model 2 were a little lower. Average LST errors of the two Models were also

Table 5
Linear regression algorithms of the simplified Model.

Range of MPDI	Algorithm equations	R^2	Accuracy evaluated by cross-validation	
			RMSE (°C)	Average LST error (°C)
<0.06	LST = 0.00104 × 6.9H + 0.01801 × 18.7V − 0.01151 × 18.7H − 0.00201 × 23.8V + 0.00271 × 23.8H + 56.82032	0.781	1.56	1.25
0.06–0.07	LST = 0.00110 × 6.9H + 0.00998 × 36.5V − 0.00457 × 36.5H + 52.19068	0.716	1.47	0.91
0.07–0.08	LST = 0.00122 × 6.9H + 0.01109 × 18.7V − 0.00823 × 18.7H + 0.00500 × 23.8V + 62.21144	0.716	1.92	1.10
0.08–0.09	LST = 0.01496 × 36.5V − 0.00720 × 36.5H + 52.18968	0.757	1.89	1.10
0.09–0.12	LST = 0.01783 × 18.7V − 0.00922 × 18.7H + 58.03248	0.818	1.84	1.30

a bit higher (1.66 and 1.34 °C, respectively) compared to Model 3 (1.00 °C). Model 3 is more complicated than the other two. We intend to develop a simpler yet effective LST retrieval model based on the three Models (Models 1, 2 and 3).

3.2. Proposed simplified LST simulation model and accuracy analysis

Comparing Tables 2–4 together, we can say that it is an effective way to derive LST based on the land surface vegetation cover classification using AMSR-E 6.9 GHz MPDI. On the whole, as the MPDI interval becomes smaller and smaller, the LST retrieval models are getting more and more accurate. However, there are no obvious improvements on algorithmic accuracies where land surfaces are covered by dense vegetation (MPDI < 0.06) and bare soil (0.09 < MPDI < 0.12). But the accuracies of regression algorithms for sparse vegetation cover areas (0.06 < MPDI < 0.09) are greatly improved when the MPDI interval reached 0.01 (average LST error: from about 1.8 to 1.04 °C). This is because in these areas the land surface is a mixture of bare soil and small vegetation (Julien et al., 2006; Mao et al., 2007a,b). Since it is difficult to develop an effective algorithm for such areas when MPDI interval is bigger than or equal to 0.02, we reduce the scale of MPDI interval into 0.01 to classify the land surface vegetation cover for areas where MPDI is between 0.06 and 0.09. Based on the above conclusions, we finally developed a simpler yet more effective LST retrieval model (Table 5 and Fig. 6).

Besides, scatter graphs were presented to compare LST retrieved from AMSR-E BT with Ts observed between February 2, 2008 and February 5, 2008 to evaluate the accuracy of the simplified model (Fig. 7).

Seen from Table 5 and Fig. 7, when MPDI is smaller than 0.06 or is larger than 0.09, it is unnecessary to reduce the MPDI interval anymore, and we can still build an effective linear regression algorithm for each surface cover type. However, when MPDI value is between 0.06 and 0.09, we need to divide MPDI intervals into three ranges: 0.06–0.07, 0.07–0.08 and 0.08–0.09 for establishing more accurate LST regression algorithms. Hence we develop three linear regression algorithms for each MPDI range, respectively. In this way, the RMSE of all algorithms of the simplified model can reach 1.47–1.89 °C (within 1.9 °C). The average temperature errors between Ts and LST are 0.91–1.30 °C. The results indicate that the simplified model of LST retrieval from AMSR-E BT data is almost as accurate as Model 3 and as simple as Model 1. The retrieval results were also more accurate than the results of former similar studies (Njoku, 1993; Njoku and Li, 1997; Aires et al., 2001; Mao et al., 2007a,b).

What is more, from Tables 2–5, we can clearly find that 3 bands of AMSR-E (6.9, 18.7 and 36.5 GHz) are the key channels to retrieve LST. This is because these 3 channels are low frequency bands and hardly influenced by the atmosphere effects under bad weather conditions. The contribution of 6.9 GHz band is to distinguish the land surfaces' vegetation cover conditions. However, the BT differences between 36.5V and 36.5H, 23.8V and 23.8H, 18.7V and

18.7H, 10.7V and 10.7H can also be used to compensate the influence of soil moisture and vegetation condition. Only 89 GHz is not included in this LST retrieval model. It is because 89 GHz band is more likely to be influenced by the atmosphere than other AMSR-E bands, especially under bad weather conditions. It is not an effective channel to retrieve LST from AMSR-E BT (Clara et al., 2009; Chris, 2008).

3.3. Advantages of the simplified LST model

The simplified model approach is a combination of the advantages of Models 1, 2 and 3. The accuracy of the simplified model (R^2: 0.716–0.818, RMSE: 1.47–1.92 °C, average LST error: 0.91–1.30 °C) is obviously higher than the Models 1 and 2 (Model 1, R^2: 0.686–0.797, RMSE: 1.61–1.81 °C, average LST error: 1.23–2.53 °C; Model 2, R^2: 0.477–0.881, RMSE: 1.36–2.45 °C, average LST error: 1.03–1.84 °C). Although the accuracy of Model 3 (R^2: 0716–0.846, RMSE: 1.24–1.98 °C, average LST error: 0.71–1.28 °C) is nearly the same as the simplified model. However, all AMSR-E polarization bands are required in Model 3 while only 7 polarization bands are required by the simplified model. What is more, the approach of Model 3 has to classify the land surface into 12 types vs. only 5 types needed for the simplified LST model. Obviously, the models can be applied to other similar area, but further work is needed for validation.

4. Conclusions

Based on analysis of the passive microwave radiance transfer equation, and MPDI-based surface cover classification, we built a simple yet effective LST retrieval model (average error of LST: 0.91–1.30 °C) by combining AMSR-E BT with observation temperatures. This study is one of the rare applications that use the field temperature to make regression analysis with AMSR-E BT products during a strong cold disaster period of 2008 in Southern China. It is also a referential example for using AMSR-E BT product to derive AMSR-E LST algorithms under extreme weather conditions.

On the basis of different MPDI intervals: 0.04, 0.02 and 0.01, three LST retrieval Models (Models 1, 2 and 3) with different performances in accuracies and complications were analyzed and combined to produced the improved simplified model. Authors classified the land surface into five types ranges of MPDI value are: <0.06, 0.06–0.07, 0.07–0.08, 0.08–0.09, and 0.09–0.12, respectively (corresponding to dense vegetation (<0.06), sparse vegetation mixed with bare soil (0.06–0.07, 0.07–0.08, and 0.08–0.09), bare soil (0.09–0.12)). We ignored those areas where MPDI > 0.12 (only 13 of 2,223 pixels in each AMSR-E BT file). Five linear regression algorithms were developed from each land surface type of the five MPDI ranges. The average error of LST retrieval by the simplified model is about 0.91–1.30 °C (model average at 1.13 °C) compared to the 1.03–2.53 of Model 1 and Model 2 (model average at 1.50 °C). Besides, all AMSR-E polarization bands and 12 land surface types

are required in Model 3 while only 7 polarization bands and 5 land surface types are required by the proposed simplified model approach.

It is an effective way to derive LST based on the land surface vegetation cover classification using AMSR-E 6.9 GHz MPDI method. And further, with the range of MPDI intervals becoming smaller the LST retrieval algorithms are getting more accurate. However, as MPDI intervals become smaller and smaller, there are no obvious improvements for the accuracies of algorithms where land surfaces are defined as bare soil (0.09 < MPDI < 0.12) and covered by dense vegetation (MPDI < 0.06) (shown in Models 1, 2 and 3). But the accuracies of simplified algorithms for sparse vegetation cover areas (0.06 < MPDI < 0.09) are greatly improved when the value of MPDI interval reaches 0.01. To a certain extent, this research makes up for limitations of Njoku's LST retrieval algorithm, which was less effective for bare soil areas (Njoku and Li, 1997). The accuracy of this simplified LST retrieval model is also much higher than former LST retrieval algorithms (usually $\geq 2\,^\circ$C) from passive microwave data (Njoku, 1993; Njoku and Li, 1997; Aires et al., 2001; Mao et al., 2007a,b).

This study is an attempt to use AMSR-E BT data retrieving winter LST in Southern China. Result confirms that the simplified LST simulation model based on MPDI and in situ observed temperature have the potential to gain more precise LST from AMSR-E remote sensing data. The new method can be applied to other similar regions supporting of ground observation, but needs to be further investigated.

Acknowledgements

Appendix A.

The Planck's function and its derived intermediate expressions are listed following:

$$B_f(T) = \frac{2hf^3}{c^2(e^{hf/kT} - 1)} \quad \text{(A1)}$$

$$B_f(T) = \frac{2kT}{\lambda^2} \frac{1}{1 + (hf/kT) + (hf/kT)^2 + \ldots + (hf/kT)^n} \quad \text{(A2)}$$

$$B_f(T) = \frac{2kT}{\lambda^2} \quad \text{(A3)}$$

where T is the temperature in Kelvin, $B_f(T)$ is the spectral radiance of the blackbody at T Kelvin, h is the Planck constant, f is the frequency of the wave band, c is the light speed, and k is Boltzman constant.

The definition formula of MPDI and its derived intermediate expressions are listed as following:

$$MPDI(\tau, \mu) = \frac{Tbv - Tbh}{Tbv + Tbh} \quad \text{(A4)}$$

$$MPDI(0, \mu) = \frac{\varepsilon_V - \varepsilon_H}{\varepsilon_V + \varepsilon_H} \quad \text{(A5)}$$

where h and v stand for horizontal (H) or vertical (V) polarization, respectively; $\mu = \cos\theta$; τ is the equivalent optical depth; ε_p is the soil emissivity for the p polarization.

References

Aires, F., Prigent, C., Rossow, W.B., Rothstein, M., 2001. A new neural network approach including first guess for retrieval of atmospheric water vapor, cloud liquid water path, surface temperature and emissivities over land from satellite microwave observations. Journal of Geophysical Research 106 (D14), 14887–14907.

Clara, S.D., Jeffrey, P.W., Peter, J.S., Richard, A.M., Thomas, R.H., 2009. An evaluation of AMSR-E derived soil moisture over Australia. Remote Sensing of Environment 113, 703–710.

Chris, D., 2008. The contribution of AMSR-E 18.7 and 10.7 GHz measurements to improved boreal forest snow water equivalent retrievals. Remote Sensing of Environment 112, 2701–2710.

Fily, M., Royer, A., Goitab, K., Prigentc, C., 2003. A simple retrieval method for land surface temperature and fraction of water surface determination from satellite microwave brightness temperatures in sub-arctic areas. Remote Sensing of Environment 85, 328–338.

Julien, Y., Sobrino, J., Verhoef, W., 2006. Changes in land surface temperatures and NDVI values over Europe between 1982 and 1999. Remote Sensing of Environment 103, 43–55.

Mao, K.B., Shi, J.C., Li, Z.L., 2007a. A physics-based statistical algorithm for retrieving land surface temperature from AMSR-E passive microwave data. Science in China Series D: Earth Sciences 50 (7), 1115–1120.

Mao, K.B., Tang, H.J., Zhou, Q.B., Chern, Z.X., Chen, Y.Q., Zhao, D.Z., 2007b. A study of the relationship between AMSR-E/MPI and MODIS LAI/NDVI. Remote Sensing for Land and Resources 1 (71), 27–31.

McFarland, M.J., Miller, R.L., Neale, C.M.U., 1990. Land surface temperature derived from the SSM/I passive microwave brightness temperatures. IEEE Transactions on Geoscience and Remote Sensing 28 (5), 839–845.

Njoku, E.G., 1993. Surface temperature estimation over land using satellite microwave radiometry. JPL Technical Report Server, 93-0046, pp. 1–28.

Njoku, E.G., Li, L., 1997. Retrieval of land surface parameters using passive microwave measurements at 6 to 18 GHz. IEEE Transactions on Geoscience and Remote Sensing, 1–43.

Paloscia, S., Pampaloni, P., 1988. Microwave polarization index for monitoring vegetation growth. IEEE Transactions on Geoscience and Remote Sensing 26 (5), 617–621.

Rubio, E., Caselles, V., Badenas, C., 1997. Emissivity measurements of several soils and vegetation types in the 8–14 μm wave band: analysis of two field methods. Remote Sensing of Environment 59, 490–521.

Wang, C.L., Liu, J.L., Zeng, X., Wan, R.J., 2004. Characteristics of recent 50 year's cold damage in winter in Guangdong. Journal of Natural Disasters 13 (4), 121–127.

Yang, H., Yang, Z.D., 2006. A modified land surface temperature split window retrieval algorithm and its applications over China. Global and Planetary Change 52, 207–215.